

Scientific Workshop on Nuclear Fission dynamics and the Emission of Prompt Neutrons and Gamma Rays, THEORY-3

Prompt Fission Neutron Experiments on $^{235}\text{U}(\text{n},\text{f})$ and $^{252}\text{Cf}(\text{SF})$

A. Göök^a, F.-J. Hamsch^{a,*}, S. Oberstedt^a, M. Vidali^a

^aEuropean Commission - Joint Research Centre - Institute for Reference Materials and Measurements, Retieseweg 111, B-2440, Geel, Belgium

Abstract

For nuclear modeling and improved evaluation of nuclear data knowledge about fluctuations of the prompt neutron multiplicity as a function of incident neutron energy is requested for the major actinides ^{235}U and ^{239}Pu . Experimental investigations of the prompt fission neutron emission in resonance neutron induced fission on ^{235}U are taking place at the GELINA facility of the IRMM. The experiment employs an array of neutron scintillation-detectors (SCINTIA) in conjunction with a newly designed 3D position sensitive twin Frisch-grid ionization chamber. A preparatory experiment on prompt fission neutron emission in $^{252}\text{Cf}(\text{SF})$ was undertaken to verify analysis procedures relevant for the implementation of the SCINTIA neutron detector array. The available literature data on the TKE dependence of the multiplicity show strong deviations. Therefore, effort was focused on investigating experimental factors in low efficiency neutron counting experiments that may lead to faulty determination of this dependence. Taking these factors into account a result that agree well with data from high efficiency neutron counting experiments is obtained.

© 2015 The Authors. Published by Elsevier B.V. This is an open access article under the CC BY-NC-ND license (<http://creativecommons.org/licenses/by-nc-nd/4.0/>).

Peer-review under responsibility of the European Commission, Joint Research Centre – Institute for Reference Materials and Measurements

Keywords: ^{235}U ; ^{252}Cf ; spontaneous fission; Neutron Multiplicity;

1. Introduction

Investigation of prompt fission neutron emission in fission is of particular importance in understanding the fission process. Knowledge of the properties of prompt fission neutrons, their multiplicities and energy distributions could give answers to questions related not only to the neutron emission itself, but also to questions relevant to the formation of the fission fragments, the sharing of excitation energy among them and the time scale of the process. For nuclear modeling and improved evaluation of nuclear data the knowledge about fluctuations in the prompt neutron multiplicity as a function of incident neutron energy is requested for the major actinides ^{235}U and ^{239}Pu (Lubitz and Roussin, 1999; De Saint Jean and McKnight, 2014). Fluctuations in fission fragment mass and total kinetic energy (TKE) in both isotopes have been observed in resonance neutron induced fission (Hamsch et al., 1989, 2011). Independently, fluctuations in the number of emitted neutrons have also been observed (Howe et al., 1976). In view of the fact that both neutron number and fission fragment properties have been found to vary it is necessary to study the correlations of

* Corresponding author. Tel.: +32 (0)14 571 351
E-mail address: Franz-Josef.HAMBSCH@ec.europa.eu

prompt neutron multiplicity and fission fragments properties in the resonance region (Gwin et al., 1984). Furthermore, the knowledge of the prompt neutron multiplicity as a function of mass and TKE is needed when determining post-neutron emission fission fragment mass distributions experimentally via the double kinetic energy or double velocity techniques. The impact on mass distributions due to fluctuations of the mass dependence of the neutron multiplicity as a function of incident neutron energy was investigated by Al-Adili et al. (2012). In the most severe cases the relative impact was as large as 20-30 %. Experimental investigations of the correlations of prompt fission neutron multiplicity with fragment properties in resonance neutron induced fission on ^{235}U and ^{239}Pu , are taking place at the GELINA facility of the JRC-IRMM.

2. Experimental Method

The experimental technique used to study prompt neutron emission in resonance-neutron induced fission at the GELINA facility is based on techniques pioneered by Bowman et al. (1962). The method involves extracting fission fragment masses by measurement of either velocity ($2v$) or energy ($2E$) of the two fragments, and coincident measurement of fission neutron time-of-flight at known angles with respect to the fission axis. This gives the basic information needed for reconstructing the neutron emission, cf. Fig. 1. In an experiment on prompt fission neutrons in $^{252}\text{Cf}(\text{SF})$ Budtz-Jørgensen and Knitter (1988) exploited the combination of a twin Frisch-grid ionization chamber for fission fragment properties ($2E$ technique) and a liquid scintillator for neutron detection. This serves as the basis for our experimental setup (which is described in Sect. 3) to study prompt neutron emission. The ionization chamber has a large solid angle, which not only facilitates the fragment-neutron coincidence rate, but also introduces a less biased selection of coincident events. The ionization chamber allows determining the fission fragment emission angle relative to the chamber axis. By placing the neutron detector along the chamber axis this angle coincides with the angle relative to the momentum direction of detected neutrons.

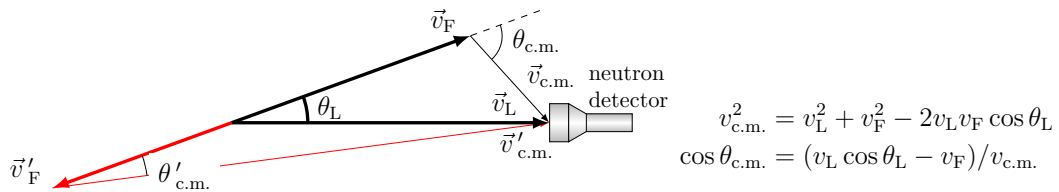


Fig. 1. (Color online) Vector diagram of the kinematics of neutron emission from a fully accelerated fragment and the transformation into the fragment rest frame (c.m.), black lines represent the fragment detected in the same hemisphere as the neutron, while red lines represent the complimentary fragment. Vectors and angles drawn with thick lines are directly measured in the experiment. The labels are; fragment velocity \vec{v}_F , complimentary fragment velocity \vec{v}'_F , neutron velocity in the laboratory frame \vec{v}_L and neutron velocity in the center-of-mass frame $\vec{v}'_{c.m.}$.

2.1. Prompt Fission Neutrons from $^{252}\text{Cf}(\text{SF})$

An experimental investigation of prompt fission neutron multiplicity correlations with fission fragment properties in the spontaneous fission of ^{252}Cf was undertaken to verify setup and analysis procedures relevant for studying neutron emission in resonance-neutron induced fission. Beside the purely experimental interest, recent advances in the theoretical description of prompt emission in fission (Lemaire et al., 2005; Becker et al., 2013; Litaize and Serot, 2010) require detailed data for verifying the models. The experiment is essentially a reproduction of the experiment performed by Budtz-Jørgensen and Knitter (1988) with the traditional analog acquisition system now replaced by a fully digital one and subsequent digital signal processing. The digital technique has shown advantages over the analog technique for fission fragment spectroscopy with a twin Frisch-grid ionization chamber (Al-Adili et al., 2010). Experimental details and main results have been published elsewhere (Göök et al., 2014), for the sake of clarity, a few selected results will be presented in the following.

In Fig. 2 the mean number of neutrons emitted per fission is shown as a function of the TKE of the fission fragments. Except for at low TKE the dependence is nearly linear. A least square fit to the data from the present experiment gives

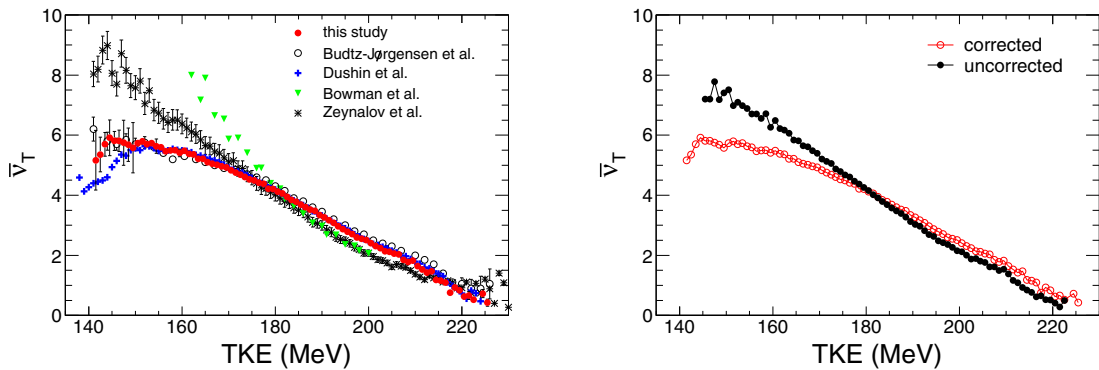


Fig. 2. (Color online) Left: Average neutron multiplicity per fission as a function of TKE, in comparison with experimental data from literature (Budtz-Jørgensen and Knitter, 1988; Bowman et al., 1963; Zeynalov et al., 2011; Dushin et al., 2004). Right: Effect of the recoil correction on the average neutron multiplicity per fission as a function of TKE in study.

an inverse slope of (12.6 ± 0.2) MeV/n. Due to the correlation between TKE and fragment mass distributions this quantity must not be interpreted as the energy needed for a pair of fragments to emit one more neutron, as noted already by Nifenecker et al. (1974). Recently, discrepancies in the available experimental data on the behavior of the total number of neutrons emitted as a function of total kinetic energy $\bar{\nu}_T(TKE)$ have been identified (Tudora, 2013; Zeynalov et al., 2011; Regnier et al., 2013), therefore efforts were made to identify experimental factors that may influence the result. All of the literature data included in Fig. 2 were extracted using similar techniques as the present study, except the data of Dushin et al. (2004) where a 4π Gd-loaded scintillator tank was used. The factor having the strongest impact on the slope of $\bar{\nu}_T(TKE)$ is the correction for recoil energy imparted to the fission fragment by the detected neutron (Gavron, 1974). The mere fact that a neutron is detected in coincidence with the fragments causes a biased selection of fission events, which needs to be corrected for. The influence of this correction on $\bar{\nu}_T(TKE)$ in the present experiment is displayed on the right hand side of Fig. 2. In an experiment covering a 4π solid angle the correction is theoretically non-existent (Nifenecker et al., 1974), it is strongest for experiments where both neutrons and fission fragments are detected in a small solid angle. This explains the deviation of the historical data

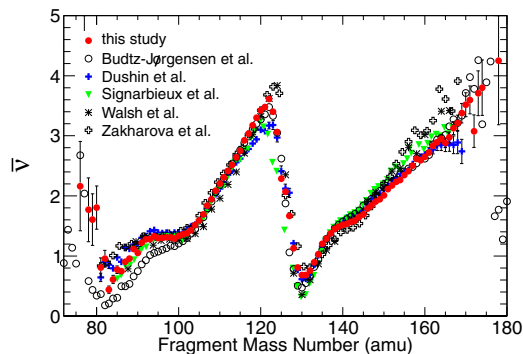


Fig. 3. (Color online) Average prompt fission neutron multiplicity as a function of fission fragment mass, in comparison with data from literature (Budtz-Jørgensen and Knitter, 1988; Dushin et al., 2004; Walsh and Boldeman, 1977; Zakharova and Ryazanov, 1979; Signarbieux et al., 1972).

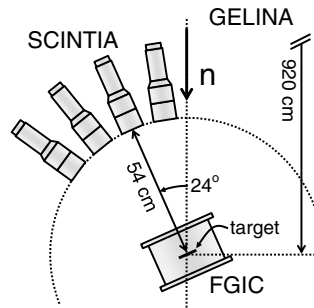


Fig. 4. Schematic view of the experimental setup.

from Bowman et al. (1962, 1963), where this was not considered. Because of the large solid angle subtended by the ionization chamber the magnitude of the correction is in our case much smaller.

The mass dependence of the prompt fission neutron multiplicity per fragment from this experiment is compared to literature data (Budtz-Jørgensen and Knitter, 1988; Dushin et al., 2004; Walsh and Boldeman, 1977; Zakharova and Ryazanov, 1979; Signarbieux et al., 1972) in Fig. 3. The data from this study agree quite well with experimental data available in the literature. More detailed discussion of the results can be found in Gök et al. (2014).

3. Setup for $^{235}\text{U}(n,f)$ Experiment

The experimental setup for investigating correlations of prompt neutrons with fission fragments in resonance-neutron induced fission on ^{235}U and ^{239}Pu is illustrated in Fig. 4. The fission target is placed inside the ionization chamber about 9.2 m away from the neutron production target of the GELINA facility. An array of neutron detectors (SCINTIA) is employed in order to facilitate the fission-neutron coincidence count rate. The SCINTIA array consists of 7 NE213 equivalent liquid scintillators (Scionix LS-301) and 5 para-therphenyl detectors. When employing an array of neutron detectors, each detector forms an axis of symmetry around which the orientation of the fission axis needs to be known. Hence the traditional ionization chamber is no longer sufficient to reconstruct the kinematics in the fragment rest frame. To remedy the situation, the ionization chamber's anode plate is replaced by a position sensitive readout structure, which allows determination of all three space components of the fission fragments' direction of travel. A 22 channel fully digital data acquisition is used. The acquisition is triggered by the current signal from the ionization chamber cathode, giving the instant of a fission event in time with a resolution better than 1 ns FWHM. For each fission event the digital waveforms of all channels, sampled at 400 MS/s with 14-bit resolution, are stored on disk for off-line treatment. A register counting the number of oscillations of the sampling clock (800 MHz) is reset by a pulse generated just before the electron bunch from the GELINA hits the neutron production target. The value of the register as the fission trigger arrives is stored together with the waveform data, giving the incident neutron time-of-flight for each event. In Fig. 5 a time-of-flight spectrum of the ongoing $^{235}\text{U}(n,f)$ experiment is displayed.

3.1. Position Sensitive Fission Fragment Detector

The position sensing structure is illustrated in Fig. 6. It consists of two parts, a plane of parallel wires and a multi-strip anode. The wire plane is placed 4 mm above the Frisch grid and the multi-strip anode is placed 4 mm further above the wire plane, with the strips oriented perpendicular to the wires. Tungsten wires of 0.025 mm radius are soldered 2 mm apart to the support structure. The support structure is a circular printed circuit board (PCB) of 17.76 cm diameter with a 10 cm \times 10 cm quadratic hole exposing the wires. Groves in the PCB were machined to form electrically insulated soldering pads. The soldering pads are connected via 100 Ω surface-mount resistors, forming a resistive charge divider with 51 resistors in total. The near and far end of the charge divider is connected to charge-sensitive pre amplifiers. The output of the charge-sensitive pre amplifiers are digitized and stored on disk for further

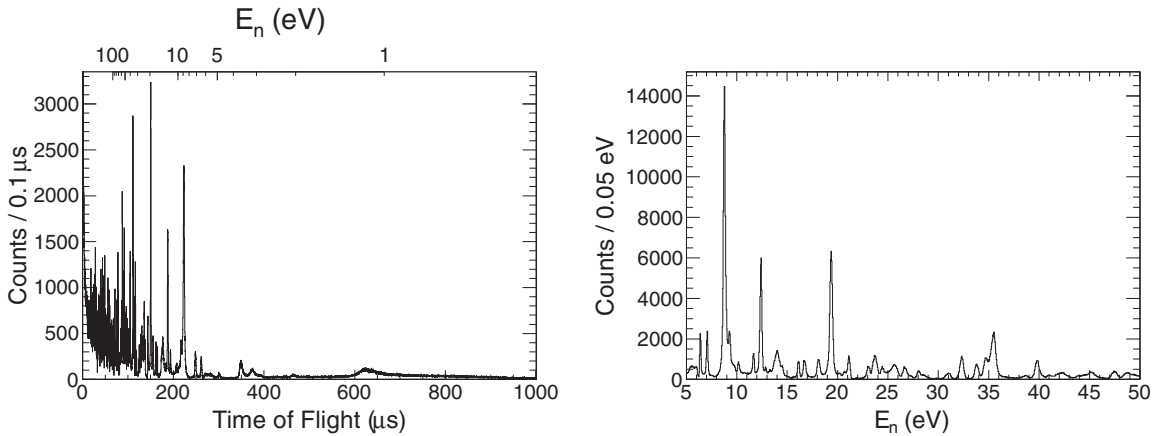


Fig. 5. Left: Incident neutron time of flight spectrum from the ongoing experiment on ²³⁵U(n,f). Right: The same spectrum converted to incident neutron energy in the range [5,50] eV (right).

treatment. The multi-strip anode consists of the same components as the wire plane except the wires themselves and the 10 cm ×10 cm quadratic hole. The construction has been tested using fission fragment from ²⁵²Cf(SF).

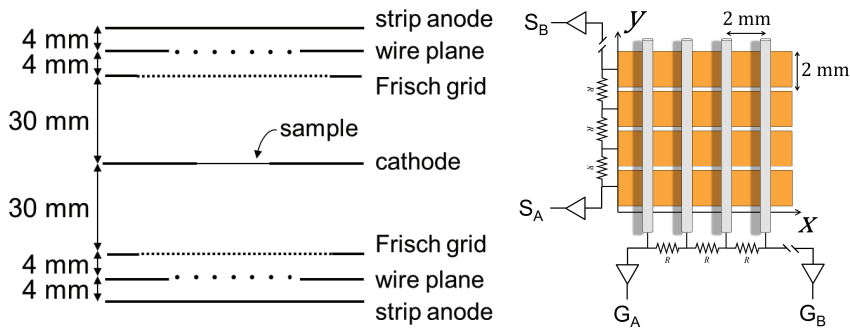


Fig. 6. Schematic view of the ionization chamber assembly and the position sensitive electrodes.

As a charged particle is stopped in the gas it leaves a trace of electrons and positive ions that proceed to drift in the electric field. The drift velocity of the positive ions is small, and can be considered as stationary during the time it takes to collect the faster drifting electrons. The Frisch grid shields the position sensing electrodes from charge induction caused by charge carriers in the ionization region. During the drift from the Frisch grid to the anode electrons induce charge on the wires closest to their drift path of the wire plane. The electrons are then collected on the individual strips of the anode, the drift time of the electron is proportional to the z-coordinate of where it was first created. Under the correct voltage conditions no electrons are collected on the wires and the final amplitude of the signals from the wire plane is zero, while the sum of the two anode signals gives the total amount of charge created by the ionizing particle. The energy resolution obtained with 4.8–5.8 MeV alpha particle is $\sigma_E/E \sim 1\%$, comparable with the standard ionization chamber resolution. The induced and collected charge on the wire plane and the anode, respectively, are divided between the near and far end pre-amplifiers giving two position figures

$$\bar{x} = \frac{P_1}{P_1 + P_2} \propto \frac{1}{n_0 e} \int x \rho(x) dx, \quad \bar{y} = \frac{A_1}{A_1 + A_2} \propto \frac{1}{n_0 e} \int y \rho(y) dy, \tag{1}$$

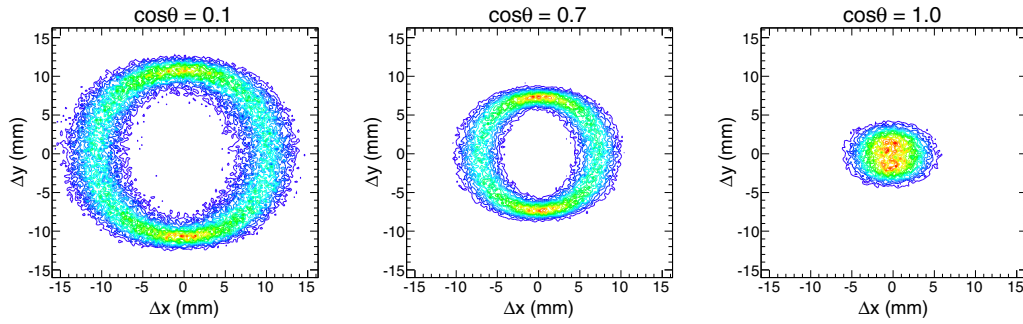


Fig. 7. Difference of the x-coordinate for complimentary fission fragments vs. the difference of the y-coordinates for three selections of the polar angle θ .

where $P_{1,2}$ are the maximum of the induced charge signals from the grid pre-amplifiers and $A_{1,2}$ are the corresponding anode signals, ρ is the charge density along the ionized track and n_0e is the total collected charge. The average electron drift time is used to determine the z -coordinate of the event (Zeynalov et al., 2012). The anode sum signal wave form is shaped using the following equation

$$t_n = \frac{1}{n_0e} \cdot \sum_{k=k_0}^{k_0+n} (q_{k+1} - q_k)(k - k_0), \quad (2)$$

where q_k is the k :th sample of the charge signal. The maximum of the resulting wave form $\{t_n\}$, reached when all electrons have been collected, gives the average drift time.

$$\bar{z} = \{t_n\}_{max} \propto \frac{1}{n_0e} \int z\rho(z)dz, \quad (3)$$

Before finding the maximum the wave form is shaped with a CRRC⁴ filter, to improve the signal to noise ratio.

The fission axis orientation in space is expressed by the polar and azimuthal angles (θ , ϕ) and the origin of the fission event on the target plane (x_0 , y_0). The polar angle is found in terms of $\cos \theta$ from the drift time, using standard procedures. The determination of the azimuthal angle is complicated by the extension of the sample material in the xy -plane. However, assuming co-linearity of the two fission fragments this difficulty can be overcome. The differences of the x and y -coordinates from the two chamber sides are independent of the location of the fission event on the target plane, and the azimuthal angle can be found from

$$\phi = \arctan \left[\frac{\bar{x}_2 - \bar{x}_1}{\bar{y}_2 - \bar{y}_1} \right]. \quad (4)$$

The quality of the \bar{x}, \bar{y} determination is illustrated in Fig. 7. Distributions of events as a function of the differences $\Delta x = \bar{x}_2 - \bar{x}_1$ and $\Delta y = \bar{y}_2 - \bar{y}_1$ for three selections of the polar angle θ are shown, circular patterns with radii proportional to $\sin \theta$ are obtained.

4. Conclusions

An investigation of prompt fission neutrons and fission fragments in the spontaneous fission of ²⁵²Cf has been performed as a preparatory step to investigate prompt fission neutron emission in resonance-neutron induced fission. A twin Frisch-grid ionization chamber was used for the determination of fission-fragment energies and masses, which also allows determining of the fission axis orientation relative to the chamber axis. Simultaneous measurement of prompt neutron time-of-flight to a scintillation detector placed at a fixed distance on the axis of the ionization chamber gives the basic information needed for reconstructing the neutron emission from fully accelerated fragments. A

literature comparison of the results show that the experimental setup and analysis is under control. Particular attention was paid to the total neutron multiplicity dependence on the TKE of the fission fragments. The main factor affecting this dependence is the treatment of the recoil energy imparted on the fission fragments detected in coincidence with a neutron, as already realized by Gavron (1974).

Prompt fission neutron and fission fragment correlations in resonance neutron induced fission on ^{235}U are taking place at the GELINA facility of the IRMM. A 3D position sensitive ionization chamber allows the determination of the fission axis orientation relative to an arbitrary axis, which makes it possible to use an array of neutron detectors, facilitating the geometrical efficiency of the setup.

Acknowledgements

The authors are grateful to the co-workers of the SN3S unit of the IRMM. The technical support of W. Geerts is particularly acknowledged.

References

- Al-Adili, A., Hamsch, F.-J., Oberstedt, S., Pomp, S., Zeynalov, S., 2010. Nucl. Instr. and Meth. A 624, 684 – 690. doi:<http://dx.doi.org/10.1016/j.nima.2010.09.126>.
- Al-Adili, A., Hamsch, F.-J., Pomp, S., Oberstedt, S., 2012. Phys. Rev. C 86, 054601. doi:10.1103/PhysRevC.86.054601.
- Becker, B., Talou, P., Kawano, T., Danon, Y., Stetcu, I., 2013. Phys. Rev. C 87, 014617. doi:10.1103/PhysRevC.87.014617.
- Bowman, H.R., Milton, J.C.D., Thompson, S.G., Swiatecki, W.J., 1963. Phys. Rev. 129, 2133–2147. doi:10.1103/PhysRev.129.2133.
- Bowman, H.R., Thompson, S.G., Milton, J.C.D., Swiatecki, W.J., 1962. Phys. Rev. 126, 2120–2136. doi:10.1103/PhysRev.126.2120.
- Budtz-Jørgensen, C., Knitter, H.H., 1988. Nucl. Phys. A490, 307–328.
- De Saint Jean, C., McKnight, R., 2014. NEA/WPEC 34.
- Dushin, V., Hamsch, F.-J., Jakovlev, V., Kalinin, V., Kraev, I., Laptev, A., Nikolaev, D., Petrov, B., Petrov, G., Petrova, V., Pl-eva, Y., Shcherbakov, O., Shpakov, V., Sokolov, V., Vorobyev, A., Zavarukhina, T., 2004. Nucl. Inst. and Meth. A 516, 539. doi:dx.doi.org/10.1016/j.nima.2003.09.029.
- Gavron, A., 1974. Nucl. Inst. and Meth. 115, 99.
- Göök, A., Hamsch, F.-J., Vidali, M., 2014. Phys. Rev. C90, 064611.
- Gwin, R., Spencer, R.R., Ingle, R.W., 1984. Nucl. Sci. Eng. 87, 381–404.
- Hamsch, F.-J., Knitter, H.H., Budtz-Jørgensen, C., Theobald, J.P., 1989. Nuclear Physics A 491, 56. doi:10.1016/0375-9474(89)90206-6.
- Hamsch, F.-J., Ruskov, I., Dematté, L., 2011. in: Proc. Scientific Workshop on Nuclear Fission Dynamics and the Emission of Prompt Neutrons and Gamma Rays (Theory-1), EUR 24802, Sinaia, Romania. p. 41.
- Howe, R.E., Phillips, T.W., Bowman, C.D., 1976. Phys. Rev. C 13, 195. doi:10.1103/PhysRevC.13.195.
- Lemaire, S., Talou, P., Kawano, T., Chadwick, M.B., Madland, D.G., 2005. Phys. Rev. C 72, 024601. doi:10.1103/PhysRevC.72.024601.
- Litaize, O., Serot, O., 2010. Phys. Rev. C 82, 054616. doi:10.1103/PhysRevC.82.054616.
- Lubitz, C., Roussin, R., 1999. NEA/WPEC 18.
- Nifenecker, H., Signarbieux, C., Babinet, R., Poitou, J., 1974. in: Proc. 3rd Symp. on Physics and Chemistry of Fission, IAEA, Vienna. p. 51.
- Regnier, D., Litaize, O., Serot, O., 2013. Nucl. Science and Engineering 174, 103–108.
- Signarbieux, C., Poitou, J., Ribarg, M., Matuszek, J., 1972. Phys. Lett. 39B, 503.
- Tudora, A., 2013. Ann. Nucl. Energy 53, 507. doi:<http://dx.doi.org/10.1016/j.anucene.2012.10.007>.
- Walsh, R., Boldeman, J., 1977. Nucl. Phys. A 276, 189.
- Zakharova, V., Ryazanov, D., 1979. Sov. J. Nucl. Phys. 30, 19.
- Zeynalov, S., Hamsch, F.-J., Oberstedt, S., 2011. Jour. Korean Phys. Soc. 59, 1396.
- Zeynalov, S., Zeynalova, O., Hamsch, F.-J., Oberstedt, S., 2012. Physics Procedia 31, 132. doi:<http://dx.doi.org/10.1016/j.phpro.2012.04.018>.
GAMMA-1 Emission of Prompt Gamma-Rays in Fission and Related Topics.